tvst

Glaucoma

The Topographic Relationship Between Choroidal Microvascular Dropout and Glaucomatous Damage in Primary Angle-Closure Glaucoma

Li Tan[1], Di Ma[1,*], Junren He[1], Hongxi Wang[1], Shirong Chen[1], and Yongdong Lin[1,*]

[1] Joint Shantou International Eye Center of Shantou University and The Chinese University of Hong Kong, Shantou, Guangdong Province, People's Republic of China

Correspondence: Yongdong Lin, Joint Shantou International Eye Center of Shantou University and The Chinese University of Hong Kong, Dong xia Road, Shantou 515041, Guangdong Province, People's Republic of China.
e-mail: lyd@jsiec.org

Received: June 9, 2022
Accepted: September 19, 2022
Published: October 14, 2022

Keywords: primary angle-closure glaucoma; optical coherence tomography angiography; choroidal microvasculature dropout; retinal nerve fiber layer thickness

Citation: Tan L, Ma D, He J, Wang H, Chen S, Lin Y. The topographic relationship between choroidal microvascular dropout and glaucomatous damage in primary angle-closure glaucoma. Transl Vis Sci Technol. 2022;11(10):20, https://doi.org/10.1167/tvst.11.10.20

Purpose: To study the topographic relationship between parapapillary choroidal microvasculature dropout (MvD) and parapapillary retinal nerve fiber layer (RNFL) defect in primary angle-closure glaucoma (PACG) eyes.

Methods: This cross-sectional study was carried out in a glaucoma clinic. Patients with PACG and healthy controls were consecutively enrolled. Each subject underwent optical coherence tomography angiography (OCTA) and OCT testing; additionally, visual field (VF) tests were also conducted in the patients with PACG. MvD was determined when choroidal layer images in OCTA showed a complete loss of the microvasculature. The study included 55 patients with PACG and 30 healthy controls.

Results: Fifty-five eyes in 55 patients with PACG and 30 eyes in 30 healthy controls were recruited. MvD was found in 26 PACG eyes (47.3%), but no MvD was found in the healthy eyes. Compared with PACG eyes without MvD, eyes with MvD had thinner average RNFL ($P < 0.001$), worse VF mean deviation ($P = 0.006$), and lower peripapillary vessel density ($P < 0.001$). Between MvD and RNFL defects, there was good topographic consistency in angular circumference (Bland–Altman 95% confidence interval [CI], −24.9° to 21.0°) and position (Bland-Altman 95% CI, −18.6° to 20.6°). There was a significant correlation between the MvD angular circumference and the average peripapillary vessel density ($r = -0.505$; $P = 0.014$), average RNFL thickness ($r = -0.742$; $P < 0.001$), and VF mean deviation ($r = -0.572$; $P = 0.004$).

Conclusions: In patients with PACG, the MvD angular circumference and position were highly topographic consistent with those of the peripapillary RNFL defect area. This study suggests that there is a significant correlation between MvD and glaucoma optic nerve injury.

Translational Relevance: Given the vascular etiology for glaucoma, the current research suggests that the MvD angular circumference may serve as a potential supplementary clue of glaucoma disease severity.

Introduction

Primary angle-closure glaucoma (PACG) is a disease that seriously threatens eyesight. It is estimated that, by 2040, about 32.04 million people in the world will have visual impairment due to PACG.[1] The main mechanisms of glaucomatous optic neuropathy are mechanical compression and insufficient blood supply.[2,3] There is growing evidence that vascular dysfunction plays a role in the pathogenesis of glaucoma,[2,4] which can be non-invasively and accurately measured using optical coherence tomography angiography (OCTA).[5–7] Recently, some studies have found that the vessel density (VD) in the optic nerve head, the peripapillary retina, and the macula decreased, and the decreasing extent was closely related to the visual field (VF) defect in PACG.[6,8–11] However, these studies examined only the superficial retinal density supplied by the central retinal artery.

More attention has been paid to peripapillary choroidal microvessels and, upstream, the posterior ciliary artery, as anatomically the posterior ciliary artery perfuses the prelaminar and laminar regions of the optic nerve head.[12–15] Traditionally, choroidal microvessels have been assessed using indocyanine green, and recently Lee et al.[16] confirmed that the parapapillary choroidal microvasculature dropout (MvD) found by OCTA is consistent with that of indocyanine green. Therefore, OCTA could be used to analyze choroidal MvD in glaucomatous patients.[17,18] So far, there is little literature regarding MvD in glaucoma. Lee et al.[19] found a topographic association between MvD location and parapapillary retinal nerve fiber layer (RNFL) defects in patients with primary open-angle glaucoma (POAG). However, no research has reported a topographic relationship between MvD and RNFL defects in PACG eyes. Furthermore, a study on POAG showed that the MvD angular circumference was significantly related to the severity of VF defect and peripapillary VD.[20] It would be of great interest to determine the correlation between glaucoma severity factors and MvD.

The purpose of this study, therefore, was to study whether MvD has a topographic association with RNFL defects. In addition, the correlation between glaucoma severity factors and MvD was evaluated.

Materials and Methods

Patients with PACG were consecutively included in the investigation of glaucomatous vascular factors, which was a study of patients with glaucoma that was conducted by the glaucoma clinic of the Joint Shantou International Eye Center (JSIEC). A healthy control group was recruited from patients who went to the JSIEC for early cataracts. We told each subject the purpose of the study, and the study protocol was approved by the Ethics Committee of JSIEC of Shantou University and the Chinese University of Hong Kong (EC20200609[6]-P19). The study followed the tenets of the Declaration of Helsinki. Written informed consent was obtained from all subjects.

All participants underwent comprehensive ophthalmic examinations that included intraocular pressure (IOP) measurement, best-corrected visual acuity, axial length measurement by OA-2000 (Tomey Corporation, Nagoya, Japan), ophthalmoscopy, swept-source OCT, and OCTA (DRI OCT Triton; Topcon Corporation, Tokyo, Japan). We used the same DRI OCT instrument to perform OCT and OCTA scans. Glaucomatous patients underwent standard VF examination by the static automated white-on-white threshold 24-2 Swedish Interactive Threshold Algorithm (SITA) standard strategy (Humphrey Field Analyzer HFA II 750i; Carl Zeiss Meditec, Zena, Germany). The systolic blood pressure (SBP) and diastolic blood pressure (DBP) of the subjects were measured before OCTA was performed. The ocular perfusion pressure was estimated as the difference between 2/3 mean arterial pressure and IOP. Mean arterial pressure was derived as 1/3 SBP + 2/3 DBP.[17]

PACG was defined as occludable anterior chamber angles in two or more quadrants on gonioscopy, as well as glaucomatous optic nerve head changes (focal or diffuse neuroretinal rim thinning, localized notching, or nerve fiber layer defects) with correlating reliable VF defects.[21] Inclusion criteria for healthy eyes included intraocular pressure $\leq$ 21 mmHg, no family history of glaucoma, normal anterior and posterior segment and non-glaucomatous optic discs as determined by clinical examination by experts. Exclusion criteria included age $\leq$ 18 years old; $\geq$6.0 D (sphere) or 3.0 D (cylinder); previous eye surgery or ocular laser surgery (except for uneventful cataract surgery or glaucoma surgery) or intraocular diseases (e.g., diabetic retinopathy or non-glaucomatous optic neuropathy) that could influence the study results; and acute angle-closure glaucoma.

OCTA Image Acquisition

In the current study, OCTA was used to study the peripapillary microvasculature circulation of continuous patients with PACG. All subjects were examined by 4.5-mm $\times$ 4.5-mm OCTA optic disc scans. We used OCTA ratio analyses of the device to obtain the images. The system automatically divided the optic disc into four layers, and the selected layer was the choroidal layer. The choroidal microvasculature in the peripapillary area was evaluated in this layer. The choroidal layer extends from the retinal pigment epithelium to 390 mm below Bruch's membrane, which is sufficient to include the full thickness of the choroid and the inner scleral surface.[18] We reviewed and filtered image quality after each scan. Images with significant motion artifacts, poor signal strength, or poor image clarity were discarded. According to the manufacturer's recommendations, the image quality score of all OCTA images had to be greater than 40.[18,22]

Choroidal MvD is a focal sectoral capillary dropout with no visible microvascular network identified in the choroidal layer images.[16,23] When the circumferential width of the area with capillary dropout appeared to be more than one-half clock hour of

the disc circumference, it was considered a disruption of the microvascular network and was deemed to be MvD.[18] Two independent researchers (JH and HW) identified MvD without knowing the clinical information for each participant. Disagreements between the researchers were resolved by a third adjudicator (DM).

For the measurement of peripapillary VD, we used Image J (National Institutes of Health, Bethesda, MD) to process the OCTA images. Peripapillary VD measurements were calculated in the nerve head layer, as described previously.[8] First, we applied a non-local means denoising filter to reduce the background noise of the grayscale images. Then, we applied Phansalkar for our adaptive local thresholding method. This method was used as the binarization algorithm for the OCTA images to obtain vascular signals as white regions and to digitize these areas. The VD value was defined as a proportion of the vessel signal in the area of interest. A previous study has proved the reproducibility of this VD analysis method.[24] The peripapillary region was a 750-mm-wide annular region of interest centered on the optic disc, with an inner diameter of 1.95 cm and an outer diameter of 3.45 cm. The peripapillary region was divided into four equal quadrants: superior, inferior, temporal, and nasal.

Measurement of Angular Circumference and Location of Peripapillary MvD and RNFL Defects

We used Photoshop CC (Adobe Systems, San Jose, CA) to measure the related parameters on the images. First, the angular circumference and location of the RNFL defects were evaluated using OCT peripapillary RNFL scans. A RNFL defect was defined as an area with a thickness of <1% of the limit of the normative database (Fig. 1, red color), as previously described.[19] Each RNFL defect was determined on the x-axis of the temporal–superior–nasal–inferior–temporal graph, and the extent of the RNFL defect was the angular width between the starting point and the ending point of the RNFL defect (α) (Fig. 1F). The location of the RNFL defect was defined as the angular position of the midpoint of the RNFL defect from the foveal–disc axis (β). The optic disc center was determined as the point where the long axis and short axis of the disc crossed, as has been done in previous studies.[20,25] The foveal–disc axis was obtained by infrared imaging provided in the OCT disc scans (Fig. 1A). To measure the MvD angular circumference, we connected the disc center to the circumferential borders of MvD, and the angle between these two lines was defined as the MvD angular circumference (γ) (Fig. 1C). A line equally bisecting the angular circumferential margins of the MvD was drawn, and the MvD location was defined as the angular position of this line from the foveal–disc axis (δ) (Fig. 1D). As described in previous literature, the foveal–disc axis in OCTA images was determined by superimposing and manually aligning the OCTA images on the infrared fundus image.[18]

The manual measurement of angular circumference and the location of any MvD or RNFL defect was repeated two times by two researchers (JH and HW), who were blinded to the participants' clinical information. The final metrics of the MvD and RNFL defect were taken as the average of the results measured by two researchers to minimize the effect of inter-rater variation.

Statistical Analyses

We used SPSS Statistics 22.0 (IBM, Inc., Chicago, IL) and MedCalc 15.2.2 (MedCalc Software, Flanders, Belgium) for all statistical analyses. The Shapiro–Wilk test was performed to evaluate the normal distribution of continuous variable data. We compared the parameters between glaucomatous eyes and healthy eyes by independent t-test, nonparametric Mann–Whitney test, and χ^2 test. These methods were also used to compare PACG eyes with and without MvD.

To evaluate the relationship between MvD angular circumference and glaucoma severity, the correlations between MvD angular circumference and global and regional vascular, structural, and functional parameters, including peripapillary VD, RNFL thicknesses, and VF mean deviation (MD), were assessed using partial correlation analysis while adjusting for potential confounding parameters for the OCTA images, as well as glaucoma severity, age, axial length, and IOP. We used kappa statistics and intraclass correlation coefficients (ICCs) to evaluate inter-examiner agreement regarding the presence of MvD and measurements from the choroidal OCTA slab. Furthermore, we used Bland–Altman analysis to evaluate the topographic correlation between MvD and RNFL defects. For the topographic correlation, whether or not one eye had multiple MvDs, we analyzed the topography of each MvD and its corresponding RNFL defect. For correlation analysis, when one eye had multiple MvDs, the MvD angular circumference was determined as the sum of the angular circumferences of each MvD. $P < 0.05$ was considered statistically significant.

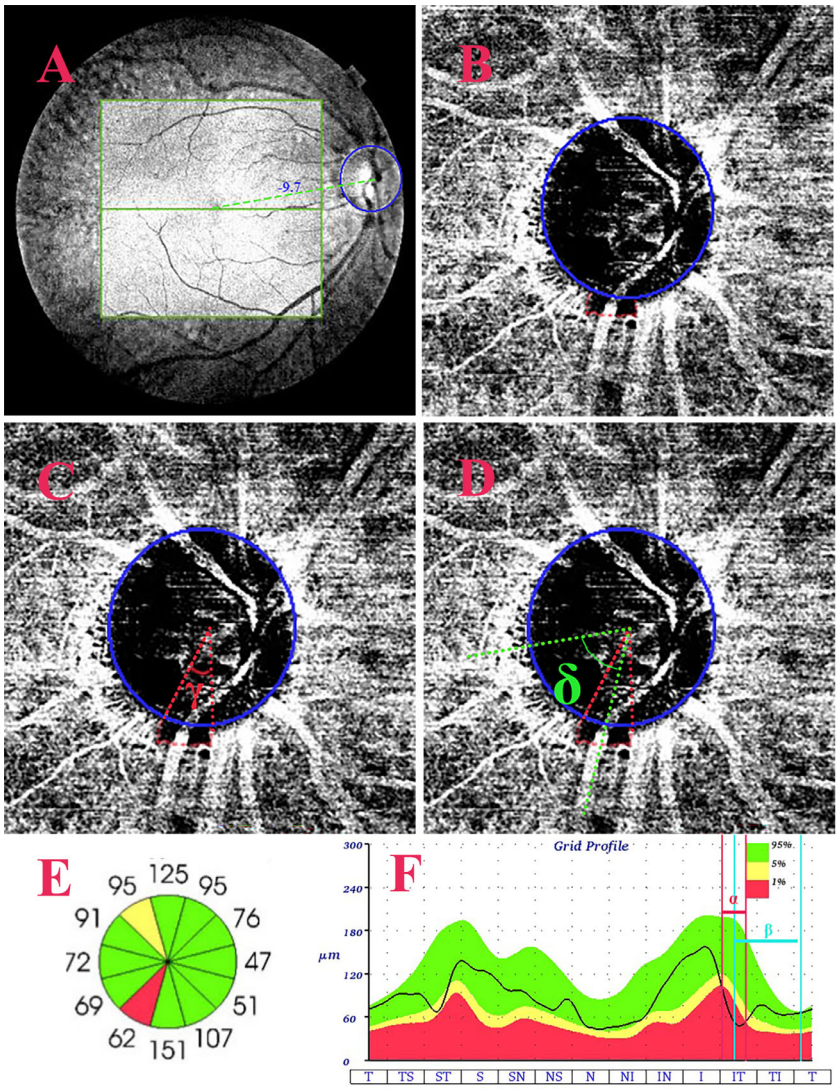

Figure 1. Measurement of the angular circumference and location of MvD and RNFL defects. (**A**) Infrared image in which the *green dotted line* indicates the foveal–disc axis. (**B**) OCTA image of the choroidal layer, where the area indicated by a *red dotted line* represents the area with MvD. (C) OCTA image of the choroidal layer, where γ is the MvD angular circumference. (**D**) OCTA image of the choroidal layer, where δ is the position of MvD relative to the foveal–disc axis. (**E**) The 12 o'clock RNFL thickness chart. (**F**) Temporal–superior–nasal–inferior–temporal RNFL thickness graph, where α is the circumferential extent of RNFL defect, and β is the position of RNFL defect relative to the foveal–disc axis.

Results

This study initially included a total of 63 PACG eyes and 32 healthy eyes. Among these eyes, eight PACG eyes and two control eyes were excluded due to poor quality of the OCTA images. The baseline characteristics of the remaining 55 PACG eyes and 30 control eyes are shown in Table 1. There was a good agreement between observers on the detection of MvD in the choroidal layer images ($\kappa = 0.915$). Twenty-six of 55 PACG eyes showed MvD (47.3%). Of the 26 eyes, two eyes and 10 eyes had single MvD in the superior and inferior hemispheres, respectively, and 14 eyes had double MvDs in the superior and inferior hemispheres. There was a total of 40 MvDs. None of the eyes in the control group had MvD. Table 2 compares the clinical features of PACG eyes with and without MvD. Compared with eyes without MvD, eyes with MvD had thinner average RNFL ($P < 0.001$), worse VF MD ($P = 0.006$), and lower peripapillary VD ($P < 0.001$). All eyes with MvD were accompanied by parapapillary atrophy (PPA), whereas eyes without PPA had no MvD.

Table 1. Baseline Characteristics of The Participants

	PACG Eyes ($n = 55$)	Healthy Eyes ($n = 30$)	*P*
Age (y)	63.2 ± 7.8	61.5 ± 8.1	0.326
Gender (male/female), *n*	21/34	8/22	0.285[a]
Axial length (mm)	22.5 ± 1.0	23.7 ± 0.9	<0.001
IOP at the scanning visit (mmHg)	14.6 ± 3.8	14.0 ± 2.9	0.360[b]
SBP (mmHg)	136.2 ± 18.9	137.3 ± 11.8	0.876[b]
DBP (mmHg)	80.7 ± 9.8	84.2 ± 7.3	0.091
Ocular perfusion pressure (mmHg)	51.5 ± 8.7	53.9 ± 6.5	0.190
Diabetes, *n* (%)	5 (9.1)	2 (6.7)	1.000[a]
VF MD (dB)	−13.4 ± 9.7	—	—
Global peripapillary VD (%)	47.0 ± 5.7	54.6 ± 2.5	<0.001[b]
Global peripapillary RNFL thickness (µm)	83.9 ± 26.9	112.7 ± 9.3	<0.001[b]

Unless otherwise indicated, values are mean ± SD and comparisons were made using the independent sample *t*-test.
[a]The comparison was performed using the χ^2 test.
[b]The comparison was performed using the Mann–Whitney test.

Table 2. Comparison of Clinical Characteristics Between PACG Eyes With and Without MvD

	PACG Eyes With MvD ($n = 26$)	PACG Eyes Without MvD ($n = 29$)	*P*
Age (y)	64.5 ± 8.2	62.1 ± 7.3	0.272
Gender (male/female), *n*	10/16	11/18	0.968[a]
Axial length (mm)	22.5 ± 0.9	22.5 ± 1.2	0.870
IOP at the scanning visit (mmHg)	15.0 ± 3.3	14.2 ± 4.2	0.440
SBP (mmHg)	136.9 ± 19.2	135.5 ± 18.9	0.786
DBP (mmHg)	81.5 ± 9.7	79.9 ± 10.0	0.540
Ocular perfusion pressure (mmHg)	51.6 ± 8.4	51.4 ± 9.2	0.919
Diabetes, *n* (%)	3(11.5)	2(6.9)	0.659[a]
VF MD (dB)	−17.1 ± 8.9	−10.1 ± 9.3	0.006[b]
Global peripapillary VD (%)	44.2 ± 4.9	49.4 ± 5.2	<0.001
Global peripapillary RNFL thickness (µm)	68.1 ± 20.8	98.1 ± 23.9	<0.001

Unless otherwise indicated, values are mean ± SD and comparisons were made using the independent sample *t*-test.
[a]The comparison was performed using the χ^2 test.
[b]The comparison was performed using the Mann–Whitney test.

Topographic Correlation Between MvD and RNFL Defects

A total of 54 RNFL defects were identified in 55 PACG eyes by OCT peripapillary scanning. Among them, 40 RNFL defects appeared in the same hemisphere as MvD. We evaluated the topographic correlation between these 40 MvDs and RNFL defects. The remaining 14 RNFL defects without MvD in the same hemisphere were not included in the topographic correlation analysis.

The intraobserver and interobserver reproducibility was high with regard to measuring the angular circumference and location of the MvD and RNFL defects. The ICCs for intraobserver reliability (JH) of the MvD angular circumference and location were 1.000 and 0.999 (95% CI, 0.998–1.000), respectively, and those for RNFL defects were 1.000 and 0.998 (95% CI, 0.996–0.999), respectively. The ICCs for interobserver reliability (JH and HW) of the MvD angular circumference and location were 0.987 (95% CI, 0.975–0.993) and 0.941 (95% CI, 0.882–0.970), respectively, and those for RNFL defects were 0.999 (95% CI = 0.999–1.000) and 0.997 (95% CI, 0.994–0.998), respectively.

The Bland–Altman diagrams of angular circumference and position in Figure 2 all show that 95% (38/40)

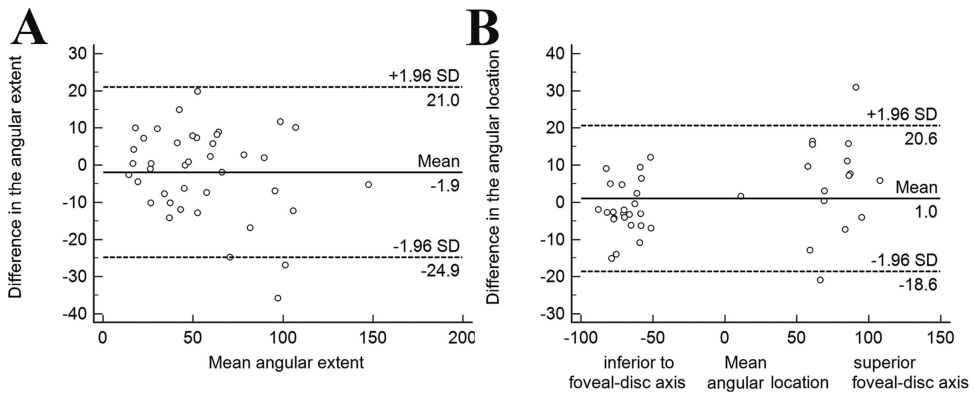

Figure 2. Bland–Altman diagrams show the angular extent (**A**) and location (**B**) of MvD versus RNFL defect. The *dashed lines* represent the 95% limits of agreement, and the *solid lines* represent the mean difference. The positive and negative values of MvD and RNFL defect locations indicate the superior and inferior positions relative to the foveal–disc axis, respectively.

Table 3. Correlations of Global and Regional VD, RNFL Thickness, and VF MD Versus Total MvD Angular Circumference Controlling for the Effect of Potential Confounders (Age, Axial Length, and IOP for 26 PACG Eyes With MvD)

	Correlation Coefficient (*r*)[a]	*P*
Global peripapillary VD (%)	−0.505	0.014[b]
Superior	−0.494	0.017[b]
Temporal	−0.353	0.099
Inferior	−0.410	0.052
Nasal	−0.373	0.080
Global peripapillary RNFL thickness (µm)	−0.742	<0.001[b]
Superior	−0.713	<0.001[b]
Temporal	−0.530	0.009[b]
Inferior	−0.465	0.025[b]
Nasal	−0.542	0.008[b]
VF MD (dB)	−0.572	0.004[b]

[a]Adjusted for age, axial length, and IOP.
[b]Values with statistical significance.

of the points were inside the 95% limits of agreement. Within the limits of agreement, the maximum absolute value of the difference between the MvD angular circumference of one eye and the corresponding RNFL defect range was 24.7° (the dot closest to the lower dotted line in the range of two dotted lines in Fig. 2A). The maximum absolute value of the difference between the MvD position of one eye and the corresponding RNFL defect position was 16.5° (the dot closest to the upper dotted line in the range of two dotted lines in Fig. 2B). Between the MvD and RNFL defects, there was good topographic consistency in angular circumference (Bland–Altman 95% CI, −24.9° to 21.0°) (Fig. 2A) and position (Bland-Altman 95% CI, −18.6° to 20.6°) (Fig. 2B). There was no significant difference between the angular circumference (55.1° ± 30.1° vs. 57.0° ± 33.0°; $P = 0.301$) and position (72.2° ± 17.7° vs. 69.1° ± 15.9°; $P = 0.537$) of the MvD and RNFL defects (paired sample *t*-test). Figure 3 shows MvD in infratemporal and supratemporal areas in the choroidal layer of a representative PACG eye and RNFL thickness defects in corresponding regions.

Correlation Between Glaucomatous Severity Factors and MvD

Table 3 shows the correlations between global and regional peripapillary VD, peripapillary RNFL thickness, and VF MD and the total MvD angular circumference in 26 glaucoma patients with MvD. There was a significant correlation between the total MvD angular

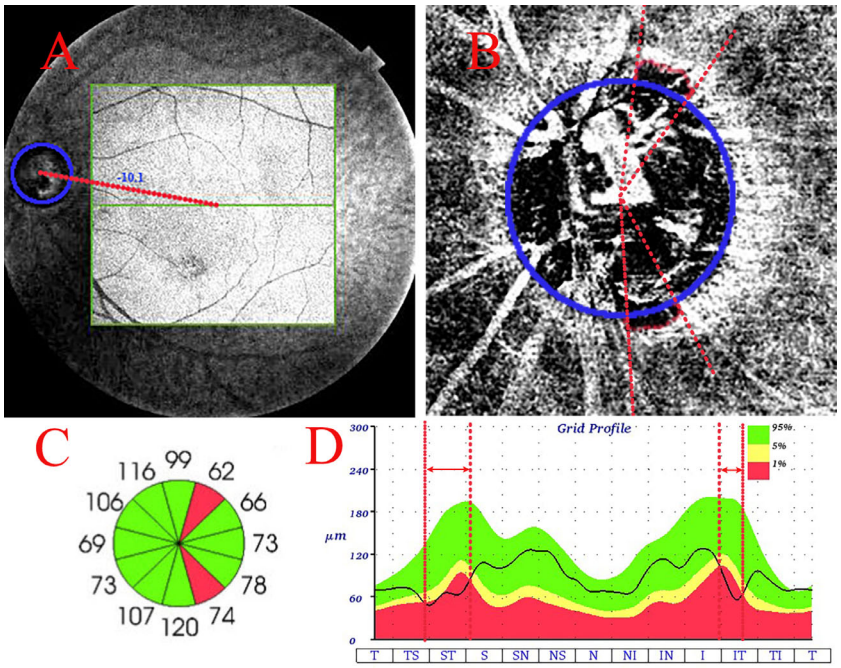

Figure 3. Example of a PACG eye with MvD in the infratemporal and supratemporal area and RNFL thickness defects in corresponding regions. (**A**) Infrared image in which the *red dotted line* indicates the foveal–disc axis. (**B**) OCTA image of the choroidal layer, where the area indicated by the *red dotted line* represents the area with MvD. (**C**) In the 12 o'clock RNFL thickness chart, the *red area* shows the corresponding RNFL defects in the supratemporal and infratemporal areas. (**D**) Temporal–superior–nasal–inferior–temporal RNFL thickness graph.

circumference and global peripapillary VD, global RNFL thickness, and VF MD (all $P < 0.05$). The MvD angular circumference was significantly correlated with peripapillary VD in the superior quadrant ($P = 0.017$) and peripapillary RNFL thickness in any sector (all $P < 0.05$).

Discussion

This study found that nearly half of patients with PACG (47.3%) showed parapapillary MvD, greater than the 35.7% found by Rao et al.[25] The possible reason may be that the severity of patients with PACG in this study (VF MD = −13.4 dB) was much higher than that in Rao et al. (VF MD = −7.8 dB). Compared with patients without MvD, patients with MvD showed more obvious glaucomatous damage, including worse VF MD, lower peripapillary VD, and thinner RNFL thickness. Previous studies in POAG eyes have reported similar findings,[19,26] indicating that the more serious the glaucomatous damage, the more likely an MvD lesion will be present. MvD may be an indicator of the severity of the disease. To the best of our knowledge, this is the first study to report that MvD has a strong topographic correlation with RNFL defects in PACG. This finding of topographic correlation concurred with the findings of Lee et al.[19] for patients with POAG, suggesting that the presence of MvD might provide clinical insight into the spatial location of RNFL damage in glaucomatous eyes.

Most MvDs have appeared in the inferotemporal quadrant, in line with our findings and suggesting that inferotemporal vascular injury might be a vulnerable zone.[17,23] We found that all eyes with MvD were accompanied by PPA, but no MvD was found in eyes without PPA, again consistent with previous studies.[16,19] It is worth noting that the previous literature has reported that PPA is related to optic disc hemorrhage[27] and the progression of glaucomatous optic neuropathy.[28–30] Lee et al.[23] used OCA to show that MvD in the parapapillary deep layers is associated with both β- and γ-zones within the areas of PPA. Furthermore, their research also showed that the microstructure of PPA with MvD is not distinguishable from that of PPA not associated with MvD. The relationship between MvD and various types of PPA in PACG was not investigated in this study but should be investigated in the future.

In 55 PACG eyes, 54 RNFL defects were found, but only 40 MvDs corresponded to them. We suspect that the artifact of superficial retinal vessels may affect the identification of MvD; however, this finding may

indicate that MvD is more likely to be secondary to the corresponding vascular occlusion after RNFL atrophy. At present, there is still no powerful evidence to indicate that MvD is one of the main causes of optic nerve damage in glaucoma or that it is secondary to reducing the blood supply because of the reduction of nutritional needs caused by optic nerve damage in glaucoma patients. However, even if MvD is secondary to the corresponding vascular occlusion after RNFL atrophy, MvD can lead to destruction of the blood–optic nerve barrier in non-perfusion areas; as a result, the released vasoactive substances or toxic substances will affect the optic nerve.[16] Therefore, greater attention should be paid to MvD by ophthalmologists. Future studies are necessary to investigate the pathogenesis of MvD and its influence on the progression of glaucoma.

In the present study, the incidence of MvD in patients with PACG was 47.3%, which was lower than the rates of 53.9% and 52.1% in POAG reported by Lee et al.[19] and Suh et al.,[17] respectively. This might suggest that the proportion of nerve damage caused by vascular factors in patients with PACG might be lower than that in POAG patients. The injury mechanisms of PACG and POAG differ. The optic nerve injury of patients with PACG may be more subject to intraocular pressure, whereas POAG patients may be more affected by vascular factors. Suh et al.[17] used OCTA to study POAG patients and found that the diastolic blood pressure of patients with MvD was lower than that of patients without MvD. In this study, we found that there was no significant difference in systolic blood pressure, diastolic blood pressure, ocular perfusion pressure, and diabetes history between patients with MvD and those without MvD. This may also indicate that the influence of vascular factors in patients with PACG is not as obvious as that in POAG patients.

Our correlation analysis of 26 glaucoma eyes with MvD showed that MvD angular circumference is significantly correlated with average peripapillary VD, average RNFL thickness, and VF MD. The correlation findings for PACG in this study are consistent with previous findings for POAG.[20] Our findings may indicate that, with development of glaucomatous injury of the optic nerve, the size of the peripapillary choroidal perfusion of the damaged PPA area in the form of MvD may increase, and the severity of the glaucomatous injury is significantly related to MvD angular circumference.

This study has some limitations. First, the artifacts of superficial blood vessels might affect the diagnosis of MvD, thus hampering precise evaluation of MvD boundaries. In the current study, the final MvD metrics included the average of four measurements made by two researchers to reduce the influence of artifacts on the results. Another limitation was that our study was a cross-sectional study and could not investigate the sequential relationship between MvD and RNFL atrophy, which will require future research. Moghimi et al.[31] reported that peripapillary VD was significantly lower in acute primary angle-closure eyes 2 months after treatment, and there was no significant change in peripapillary VD of the affected eye between 2 and 8 months after acute angle closure. The peripapillary VD of chronic angle closure decreased with progression of the disease. This article was a cross-sectional study, so it was impossible to determine the dynamic changes of peripapillary VD, which will also require future research.

In summary, this study found that MvD angular circumference and location were highly consistent with those of RNFL defect areas in patients with PACG. This study suggests that there is a significant correlation between MvD and glaucomatous optic nerve injury. Moreover, MvD angular circumference may serve as a potential clue to disease severity.

Acknowledgments

The authors thank all of the technicians and clinical research collaborators of the clinical research center at JSIEC.

Supported by the Science and Technology Project of Shantou City, Guangdong, China (200630185260914).

Disclosure: **L. Tan**, None; **D. Ma**, None; **J. He**, None; **H. Wang**, None; **S. Chen**, None; **Y. Lin**, None

* YL and DM contributed equally to this work.

References

1. Tham YC, Li X, Wong TY, Quigley HA, Aung T, Cheng CY. Global prevalence of glaucoma and projections of glaucoma burden through 2040: a systematic review and meta-analysis. *Ophthalmology*. 2014;121:2081–2090.
2. Yanagi M, Kawasaki R, Wang JJ, Wong TY, Crowston J, Kiuchi Y. Vascular risk factors in glaucoma: a review. *Clin Exp Ophthalmol*. 2011;39:252–258.
3. Nongpiur ME, Ku JY, Aung T. Angle closure glaucoma: a mechanistic review. *Curr Opin Ophthalmol*. 2011;22:96–101.
4. Flammer J, Orgul S, Costa VP, et al. The impact of ocular blood flow in glaucoma. *Prog Retin Eye Res*. 2002;21:359–393.

5. Richter GM, Chang R, Situ B, et al. Diagnostic performance of macular versus peripapillary vessel parameters by optical coherence tomography angiography for glaucoma. *Transl Vis Sci Technol*. 2018;7:21.
6. Rao HL, Kadambi SV, Weinreb RN, et al. Diagnostic ability of peripapillary vessel density measurements of optical coherence tomography angiography in primary open-angle and angle-closure glaucoma. *Br J Ophthalmol*. 2017;101:1066–1070.
7. Lin YH, Huang SM, Yeung L, et al. Correlation of visual field with peripapillary vessel density through optical coherence tomography angiography in normal-tension glaucoma. *Transl Vis Sci Technol*. 2020;9:26.
8. Lin Y, Chen S, Zhang M. Peripapillary vessel density measurement of quadrant and clock-hour sectors in primary angle closure glaucoma using optical coherence tomography angiography. *BMC Ophthalmol*. 2021;21:328.
9. Liu L, Jia Y, Takusagawa HL, et al. Optical coherence tomography angiography of the peripapillary retina in glaucoma. *JAMA Ophthalmol*. 2015;133:1045–1052.
10. Scripsema NK, Garcia PM, Bavier RD, et al. Optical coherence tomography angiography analysis of perfused peripapillary capillaries in primary open-angle glaucoma and normal-tension glaucoma. *Invest Ophthalmol Vis Sci*. 2016;57:OCT611–OCT620.
11. Lin Y, Ma D, Wang H, et al. Spatial positional relationship between macular superficial vessel density and ganglion cell-inner plexiform layer thickness in primary angle closure glaucoma. *Int Ophthalmol*. 2022;42:103–112.
12. O'Brart DP, de Souza Lima M, Bartsch DU, Freeman W, Weinreb RN. Indocyanine green angiography of the peripapillary region in glaucomatous eyes by confocal scanning laser ophthalmoscopy. *Am J Ophthalmol*. 1997;123:657–666.
13. Onda E, Cioffi GA, Bacon DR, Van Buskirk EM. Microvasculature of the human optic nerve. *Am J Ophthalmol*. 1995;120:92–102.
14. Yamazaki S, Inoue Y, Yoshikawa K. Peripapillary fluorescein angiographic findings in primary open angle glaucoma. *Br J Ophthalmol*. 1996;80:812–817.
15. Hayreh SS. The blood supply of the optic nerve head and the evaluation of it—myth and reality. *Prog Retin Eye Res*. 2001;20:563–593.
16. Lee EJ, Lee KM, Lee SH, Kim TW. Parapapillary choroidal microvasculature dropout in glaucoma: a comparison between optical coherence tomography angiography and indocyanine green angiography. *Ophthalmology*. 2017;124:1209–1217.
17. Suh MH, Zangwill LM, Manalastas PI, et al. Deep retinal layer microvasculature dropout detected by the optical coherence tomography angiography in glaucoma. *Ophthalmology*. 2016;123:2509–2518.
18. Lee EJ, Kim TW, Kim JA, Kim JA. Central visual field damage and parapapillary choroidal microvasculature dropout in primary open-angle glaucoma. *Ophthalmology*. 2018;125:588–596.
19. Lee EJ, Lee SH, Kim JA, Kim TW. Parapapillary deep-layer microvasculature dropout in glaucoma: topographic association with glaucomatous damage. *Invest Ophthalmol Vis Sci*. 2017;58:3004–3010.
20. Kwon J, Shin JW, Lee J, Kook MS. Choroidal microvasculature dropout is associated with parafoveal visual field defects in glaucoma. *Am J Ophthalmol*. 2018;188:141–154.
21. Ballae Ganeshrao S, Senthil S, Choudhari N, Sri Durgam S, Garudadri CS. Comparison of visual field progression rates among the high tension glaucoma, primary angle closure glaucoma, and normal tension glaucoma. *Invest Ophthalmol Vis Sci*. 2019;60:889–900.
22. Lee EJ, Kim TW, Kim JA, et al. Elucidation of the strongest factors influencing rapid retinal nerve fiber layer thinning in glaucoma. *Invest Ophthalmol Vis Sci*. 2019;60:3343–3351.
23. Lee EJ, Kim TW, Lee SH, Kim JA. Underlying microstructure of parapapillary deep-layer capillary dropout identified by optical coherence tomography angiography. *Invest Ophthalmol Vis Sci*. 2017;58:1621–1627.
24. Shoji T, Yoshikawa Y, Kanno J, et al. Reproducibility of macular vessel density calculations via imaging with two different swept-source optical coherence tomography angiography systems. *Transl Vis Sci Technol*. 2018;7:31.
25. Rao HL, Sreenivasaiah S, Riyazuddin M, et al. Choroidal microvascular dropout in primary angle closure glaucoma. *Am J Ophthalmol*. 2019;199:184–192.
26. Shin JW, Kwon J, Lee J, Kook MS. Choroidal microvasculature dropout is not associated with myopia, but is associated with glaucoma. *J Glaucoma*. 2018;27:189–196.
27. Jonas JB, Martus P, Budde WM, Hayler J. Morphologic predictive factors for development of optic disc hemorrhages in glaucoma. *Invest Ophthalmol Vis Sci*. 2002;43:2956–2961.
28. Leung C. Predictive factors within the optic nerve complex for glaucoma progression: disc

hemorrhage and parapapillary atrophy. *Asia Pac J Ophthalmol (Phila)*. 2012;1:187.
29. Blumberg D, Skaat A, Liebmann JM. Emerging risk factors for glaucoma onset and progression. *Prog Brain Res*. 2015;221:81–101.
30. Teng CC, De Moraes CG, Prata TS, et al. The region of largest beta-zone parapapillary atrophy area predicts the location of most rapid visual field progression. *Ophthalmology*. 2011;118:2409–2413.
31. Moghimi S, SafiZadeh M, Xu BY, et al. Vessel density and retinal nerve fibre layer thickness following acute primary angle closure. *Br J Ophthalmol*. 2020;104:1103–1108.